Mine Water Environ (2018) 37:565–576
DOI 10.1007/s10230-017-0487-8

TECHNICAL ARTICLE

Assessment and Prevention of Water and Sand Inrush Associated with Coal Mining Under a Water-filled Buried Gully: A Case Study

Gangwei Fan[1,2] · Dongsheng Zhang[3] · Shizhong Zhang[2] · Chengguo Zhang[4]

Received: 9 January 2017 / Accepted: 28 August 2017 / Published online: 2 September 2017

Abstract Mining under a water-filled buried gully risks a potentially serious water and sand inrush, especially if the bedrock is thin. A case study was conducted at a Chinese coal mine, where the thin overlying overburden was covered by widely distributed gullies. Several empirical formulas and numerical modelling indicated that the overlying strata was almost totally fractured and that all of the conditions for an inrush were met. Pre-mining dewatering and grout injection were initiated. The groundwater table was lowered by 13 surface pumping wells and 33 underground upholes that were drilled around the gully. Those located at the bottom of the gully were generally better in aquifer dewatering than those located at the banks. A barrier was constructed to avoid a water inrush by injecting a chemical grout into the bottom of the buried gully through 25 surface holes. Field observations of the water table, underground water yield, and overburden movement prove the validity of the assessment methods and treatments.

Keywords Underground mining · Buried gully · Numerical modelling · Aquifer dewatering · Grout injection

Introduction

A gully is generally formed by running water eroding sharply into soil or rock, typically in arid and semi-arid zones. When the gully is later refilled by sand or soil, a buried gully forms, which can greatly affect the local hydrogeology. Unconfined water can rush into the buried gully and into the groundwater reservoir. Such scenarios are common in northwest China, where the surface is almost desert and shallow coal seams are widely distributed under the gullies. The proven coal reserve in northwest China accounts for four-fifths of the nation's coal. Surface slope sliding can occur due to the effects of underground mining (Benko and Stead 1998; Lai et al. 2015; Marschalko and Treslin 2009; Stead and Benko 1998; Tang 2009; Wang et al. 2013). However, the same erosion that caused the gully has often thinned the rock strata above the coal seam. Previous studies and experience in underground mining of shallow seams under gullies has revealed that surface slope sliding can cause a rock burst due to shock loading, and that such shallow underground mines are also in serious danger of water and sand inrush (Fan et al. 2009; Tang 2009; Wang et al. 2011; Zhang et al. 2012).

In total extraction of a shallow coal seam, mining-induced fractures in the overburden create pathways for overlying water or sand to drain into the mine, with the consequent threat to mine safety and productivity (Kesserû 1995; Li et al. 2002; Li and Zhou 2006; Wu and Zhou 2008). For example, in 1996, coalface #1203 of the Daliuta Mine, where the overlying bedrock was 15–30 m thick, was submerged by water and sand in 4 days; in 1990, water and sand

Electronic supplementary material The online version of this article (doi:10.1007/s10230-017-0487-8) contains supplementary material, which is available to authorized users.

✉ Dongsheng Zhang
zdscumt@126.com

[1] Key Laboratory of Deep Coal Resource Mining, Ministry of Education of China, China University of Mining and Technology, Xuzhou 221116, China

[2] School of Mines, China University of Mining and Technology, Xuzhou 221116, China

[3] State Key Laboratory of Coal Resources and Safe Mining, China University of Mining and Technology, Xuzhou 221116, China

[4] School of Mining Engineering, University of New South Wales, Sydney 2052, Australia

inundated coalface #22,402 of the Halagou Mine, where the overlying bedrock was 29.5–64.70 m thick (Fan 1996).

In order to evaluate the disturbance of longwall mining on the overburden strata, four zones in order of severity from the immediate roof toward the surface, were defined, as follows: caved zone, fractured zone, continuous deformation zone, and soil zone (Peng 2008). The strata in the caved zone are broken into irregular but platy shapes of various size; the strata in the fractured zone are broken into blocks by vertical and/or subvertical fractures and horizontal cracks due to bed separation; the strata in the continuous deformation zone deform gently without causing any major cracks that extend long enough to cut through the thickness of the strata. Based mainly on groundwater aspects, Kendorski (1993, 2006) divided the overburden into caved zone, fractured zone, dilated zone, constrained zone, and surface zone. The water in the caved zone or fractured zone will drain to the mine; the dilated zone has increased storativity with little or no vertical transmissivity; whilst the water in the constrained zone is unaffected (Kendorski 1993, 2006; Peng 2008; Singh and Atkins 1983; Tieman and Rauch 1987). Booth (2002) proposed that the most important hydrological division of the overburden was into three zones, the intensely fractured zone, intermediate zone, and near-surface fractured zone. Tammetta (2013) proposed that the longwall caving process creates two distinct zones above a continuously sheared panel: the collapsed zone, which is severely disturbed and is completely drained of groundwater during caving, and the disturbed zone, in which the hydraulic heads remain relatively stable except for the immediate lowering associated with drainage of lower strata and minor increases in void space after caving.

Generally, water inrush occurs when the aquifer or water body falls into caved and fractured zones (Singh 1986; Zhang and Shen 2004; Zhang and Peng 2005). Sand inrushes are highly associated with water inrushes, which carry the sand into the mine (see Fig. 1) (Qian et al. 1994, 1996). If all the following appear, the surface or sub-surface sand can be expected to enter the mine: (1) a thick, saturated, sandy aquifer (the finer the sand, the easier it flows); (2) a pathway (the fractures in the caved and fractured zones); (3) a large space for storing water and sand (goaf); (4) an initial force driving the sand flow (gravity and water pressure).

The potential impact of mining-induced groundwater flow on an underground mine should be assessed at the prefeasibility stage through a desk study and primary geological investigations (Morton and Van Mekerk 1993). Coal mining below the ocean, lake, river, or aquifers has been successfully carried out by caving methods in many parts of the world (Gandhe et al. 2005). If the water and sand inrush occur according to the assessments, the mining engineers have to make a choice between not extracting the coal or taking measure(s) to lower the threat of an inrush. Options

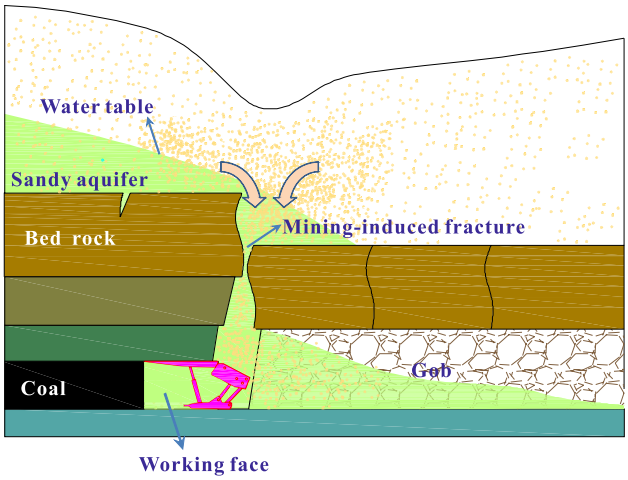

Fig. 1 The mechanism by which underground mining leads to water and sand inrush

available are dewatering, diversion, sealing, or a combination of these (Morton and Van Mekerk 1993). This paper reports a case study in the underground Daliuta Mine in the Shendong coalfield, where shallow coal seams and gullies are widely distributed.

Geology and Panel Layout

Longwall panel #12,404 of the Daliuta Mine is 5241 m in length and 220 m in width. The surface is covered by 2–35 m of Quaternary aeolian sand. Gravel of 2–40 mm in particle size lies at the bottom of the alluvial sandy layer. The Muhe Gully, which is about 80 m wide and 40 m deep, cuts through the ground surface above panel #12,404. There is a buried gully beneath the Muhe Gully (see supplemental Fig. 1). Figure 2 shows a cross section of the buried gully at its deepest point. The buried gully cuts through about 10 m of the overburden strata, which is dominated by sandstone and sandy mudstone, over a width of about 40 m. The water depth in the buried gully exceeds 14 m, which is potentially catastrophic to underground mining. The static-storage of the groundwater in this gully zone reaches 25,303 m^3. A 4.0-m-thick coal seam, numbered 2^{-2} seam, which is nearly flat, is buried at a depth of 40–95 m. Due to the gullies, the minimum thickness of overburden rock strata above the coal seam is only 18.2 m. Figure 3 shows the comprehensive geological column of the overlying strata.

Empirical Assessment

Many existing empirical formulas can be used to predict the possibility of water inrush occurrences (Zhang and Shen

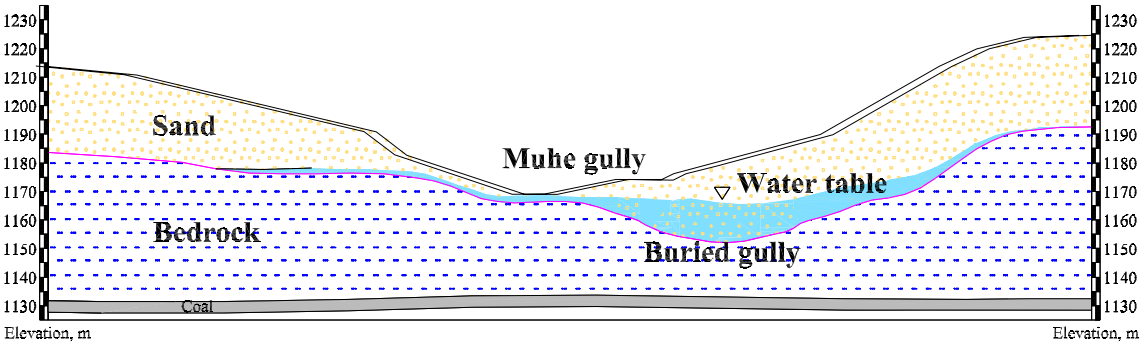

Fig. 2 Cross section of a buried gully

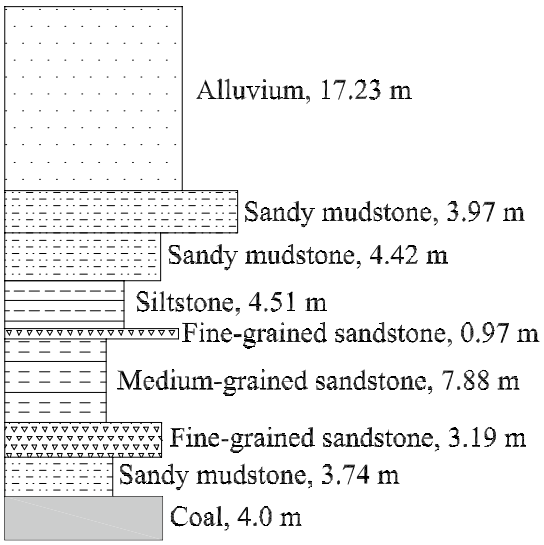

Fig. 3 The comprehensive geological column for the overlying strata

2004) based on the seam depth. The U.K. National Coal Board (1975) recommended a maximum tensile strain of 10 mm/m to govern the minimum seam depth or thickness of the interburden between the water body and the mined seam, say 67.5 t (where t represents the mining height). In the USA, the minimum seam depth is defined as 60 t (Singh and Atkins 1983). Substituting 4.0 m for t in this case, the minimum interburden thicknesses would be about 270 and 240 m, respectively. Apparently, the calculated interburden thickness for avoiding a water inrush is several times the actual overburden thickness, which is 18.2–35.8 m in this case, which indicates that total extraction of coal under a water-filled buried gully is highly risky.

The height of the fractured zone is also widely used as an important index to assess the risk of water inrush. Generally, the height of the fractured zone ranges from 20 to 50 times the mining height (Booth 2002; Kendorski 2006; Peng 2008). Based on field data from more than 200 boreholes in 27 mine sites, Liu (1981) developed the following empirical formula, which is often employed for predicting the height of the fractured zone in China.

$$H_f = \frac{100M}{aM + b} \pm \delta \tag{1}$$

where H_f is the height of the fractured zone, m; M is the mining height (4.0 m in this case); a and b are coefficients that depend on the strata lithology and strength (1.6 and 3.6, respectively, in this case); and δ is the mean square deviation, 5.6 in this case (Liu 1981; Miao et al. 2011). Therefore, the minimum predicted height of the fractured zone is about 40 m, which exceeds the overburden strata thickness; therefore, the water in the buried gully may flow into the goaf through the mining-induced fractures.

Sand movement is highly related to water head. When the water head exceeds a critical value, sand may be carried by the water and inundate the goaf, providing that the overlying rock is fractured. The water head at the time sand starts to move is called the critical water head. If the actual aquifer thickness is greater than the critical value, sand inrush may occur. Wu and Lu (2004) described the relation between the critical thickness of sand aquifer thickness and the sand thickness with the following equation:

$$h = \frac{0.44\gamma_s h_s}{\gamma(1 + 0.44)} \tag{2}$$

where h is the critical aquifer thickness; h_s is the sand thickness (2 to 35 m in this case); γ_s is the specific weight of sand, 1.48×10^4 N/m^3; and γ is the specific weight of water, 0.98×10^4 N/m^3. Therefore, the critical aquifer thickness in this case was 0.92–16.15 m, corresponding to the sand thickness. The actual aquifer thickness was 2–15.3 m, which indicated that the underground mine in this zone was in danger of a sand inrush.

Numerical Modelling

Although empirical formulas can be easily used to assess the risk of water inrush, they are site-specific and do not take the topography into consideration. Numerical modelling is widely used for coal mine ground control assessment and design (Peng 2008). A commercial software, UDEC (Universal Distinct Element Code), which is based on the finite element method, is often used for simulating fractured rock and was used to evaluate overburden failure development (Gandhe et al. 2005; Morsy and Peng 2002; Saeedi et al. 2013; Zhang and Sanderson 1998).

Model Setup

A UDEC model (Fig. 4) was established based on the stratigraphic sequence shown in Fig. 3 and the properties of the different layers (Table 1). All the rocks in the model were assumed to follow the Mohr–Coulomb failure criterion. The model is solved in two steps: (1) geostatic, the in-situ stresses are initialized in the model; (2) retreat mining, to model the mining sequences in longwall mining, using a cutting web of 5 m in the model. The model grids are shown in Fig. 4. The right boundary of the model corresponds to the actual site at a distance of 2050 m from the setup room in which the horizontal displacement was set as a constraint in the model. The horizontal displacement of the left boundary was also fixed in horizontal displacement. The bottom boundary was fixed both in both vertical and horizontal displacements. The top boundary was free.

Model Calibration

The accuracy of numerical models depends on the reliability of the input parameters. Therefore, model calibration is indispensable for realistic predictions (Peng 2008). Quantitative validation was conducted by comparing the modelling

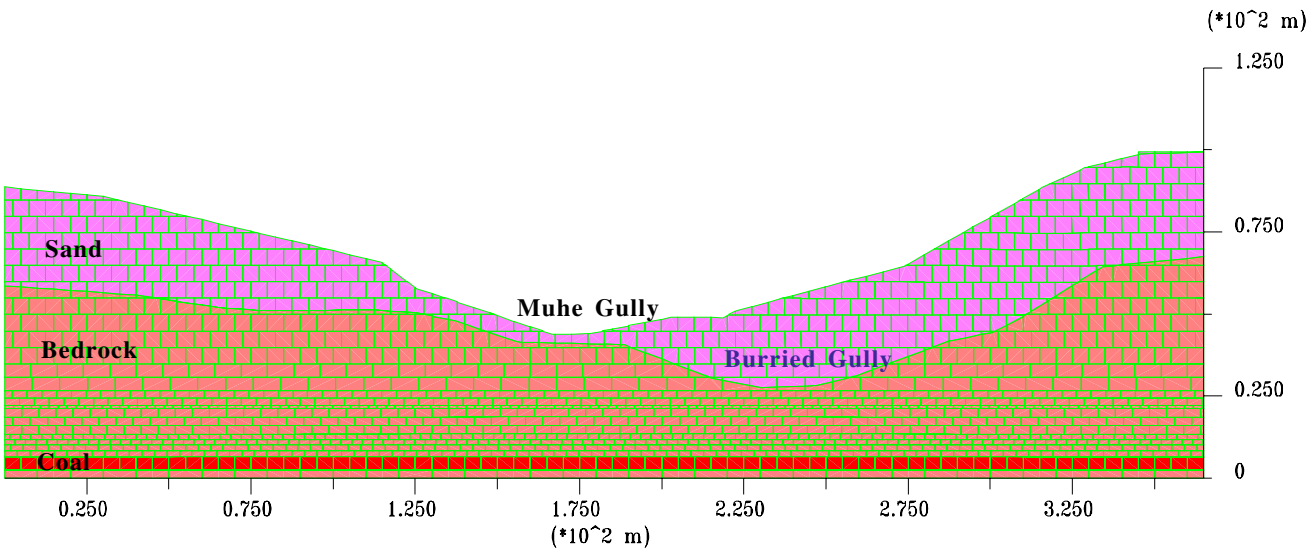

Fig. 4 The original grids of the UDEC model

Table 1 Mechanical properties of rock used in the UDEC model

Rock layer	Density (kg/m^3)	Bulk modulus (MPa)	Shear modulus (MPa)	Internal angle of friction (°)	Tensile strength (MPa)
Sand	1650	80	80	15	0.1
Sandy mudstone	2470	230	200	32	1.5
Sandy mudstone	2540	280	260	34	2.0
Siltstone	2630	360	350	32	2.2
Fine-grained sandstone	2680	420	360	38	3.8
Medium-grained sandstone	2590	340	300	36	3.1
Sandy mudstone	2630	300	260	30	2.5
Coal	1360	180	135	28	1.0

surface subsidence of three selected points against the field measurements.

Three monuments for surface subsidence measurement were placed at the boundary of the study area, A, B, and C. The modelling results and field data are compared in Fig. 5. The maximum error is about 7.55%, which indicates that the modelling results correlate well with the field measurements. Therefore, the model is a reasonable approach for predicting overburden movement.

Modelling Results

Two UDEC plots, at retreats #13 and #26 (the distances from the face to the right boundary are 65 and 135 m, respectively), are shown in Fig. 6. All the bed strata are highly fractured in the goaf where intensive fracturing and yielding were observed, although the exact height of the caved zone is not accurate due to differential loading from the sand cover. For retreat #13, the height of the caved zone reaches 20.3 m, which was 5.08 times the mining height; for retreat #26, the height of the caved zone is 15.8 m, which was 3.95 times the mining height. The sandy aquifer is thus connected to the mine void by mining-induced fractures.

Assessments

In this case, water and sand inrush heavily threatens underground mining according to both the empirical analysis and UDEC modelling. The thin bedrock, especially at the buried gully zone (18.2 m at the thinnest), is part of the intensely fractured zone, which provide sufficient pathways for water and sand flow. All four of the above-mentioned circumstances causing water and sand flow are present in this case. Therefore, special measures must be taken for mining safety when the coalface is beneath the buried gully.

Preventive Measures

Sand inrush incidents are highly associated with water inrush. Therefore, preventing a water inrush was essential. Groundwater can be either removed or diverted to avoid a

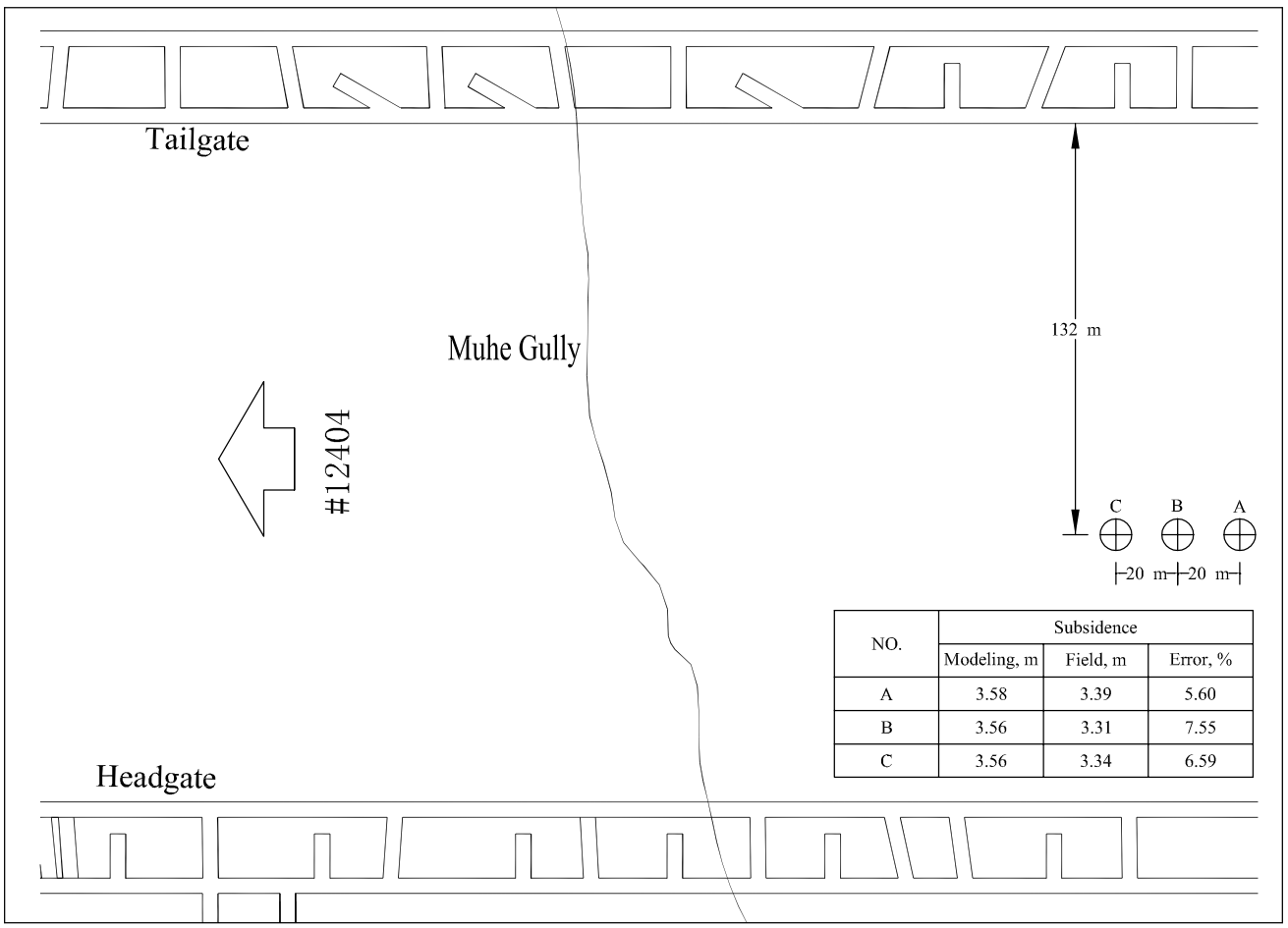

NO.	Subsidence		
	Modeling, m	Field, m	Error, %
A	3.58	3.39	5.60
B	3.56	3.31	7.55
C	3.56	3.34	6.59

Fig. 5 A comparison between the modeling results and field data

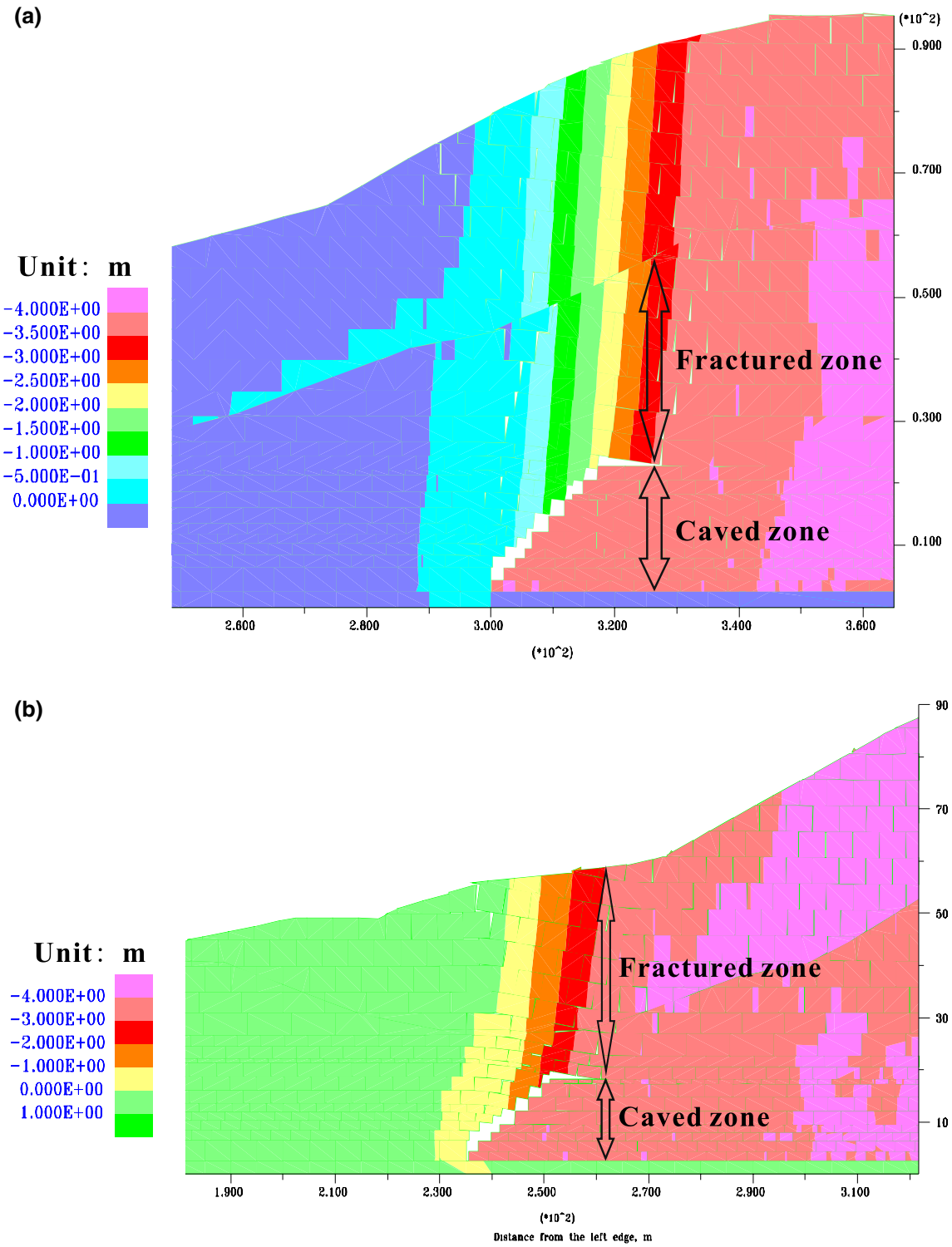

Fig. 6 The strata movement response to underground mining: **a** retreat #13; **b** retreat #26

water inrush; otherwise, it can be sealed off from workings cost effectively (Morton and Van Mekerk 1993). In this case, the groundwater should be lowered and the potential pathways should be sealed prior to and during the mining operation.

Pre-mining Dewatering

Surface pumping wells and underground upholes were drilled around the gully to remove the groundwater and lower the water table. 13 pumping wells of 600 mm in

diameter were drilled from the ground surface to the bottom of the weathered strata; 33 underground upholes, 108 mm in diameter, nearly 20 m apart, were drilled at 65°-70° inclined to the horizontal from the headgates and tailgates to the gravel. The locations of wells and boreholes are shown in Fig. 7. Two monitoring boreholes for water table logging, 220 mm in diameter, were drilled from the surface to the top of bedrock. On July 17, 2012, the underground coalface entered the buried gully area, and on July 24, the coalface passed the gully.

The flow rates in the 13 pumping wells were observed once a day from June 1 to July 24 (Fig. 8), and totaled 50,282 m^3 in 54 days. The flow rates in all 13 wells was less each day, and decreased especially when the coalface was beneath the buried gully. The initial flow rates ranged from 0.98 to 25.36 m^3/h, 7.85 m^3/h on average; on July 17, the maximum flow rates in the wells changed to 4.36 m^3/h, with an average value of 1.48 m^3/h; on July 24, the flow rates approached 0 m^3/h. Generally, the flow rates in the wells located at the bottom of buried gully, such as #5, #10, #11, and #12, were greater than those in the wells located at the banks, such as #1, #2, and #3. The flow rates in most of the wells at the banks were less than 5 m^3/h during the pumping time period.

Flow rates in the 33 underground upholes were monitored three times a day (Fig. 9). The initial flow rates ranged from 0 to 18.33, 1.80 m^3/h on average; the values on July 17 ranged from 0 to 9.02, 0.79 m^3/h on average; on July 23, the maximum flow rate was 8.12 m^3/h, with an average of 0.71 m^3/h; on Aug 7, the maximum was 2.67 m^3/h, and the average was 0.40 m^3/h. The total water discharge volume from the 33 upholes totaled 51,273 m^3 in 48 days. The water discharged from the boreholes around the buried gully accounted for 92.6% of the total volume. Generally, the flow rates in the boreholes located at the bottom of buried gully, such as TS7, were greater than those in the boreholes located at the banks, such as TS8, T2. TS7, and TS18 had much higher flow rates than any of the other holes, including those located in the gully, such as T3 and T31. The flow rates of all upholes at the banks were almost all less than 4 m^3/h.

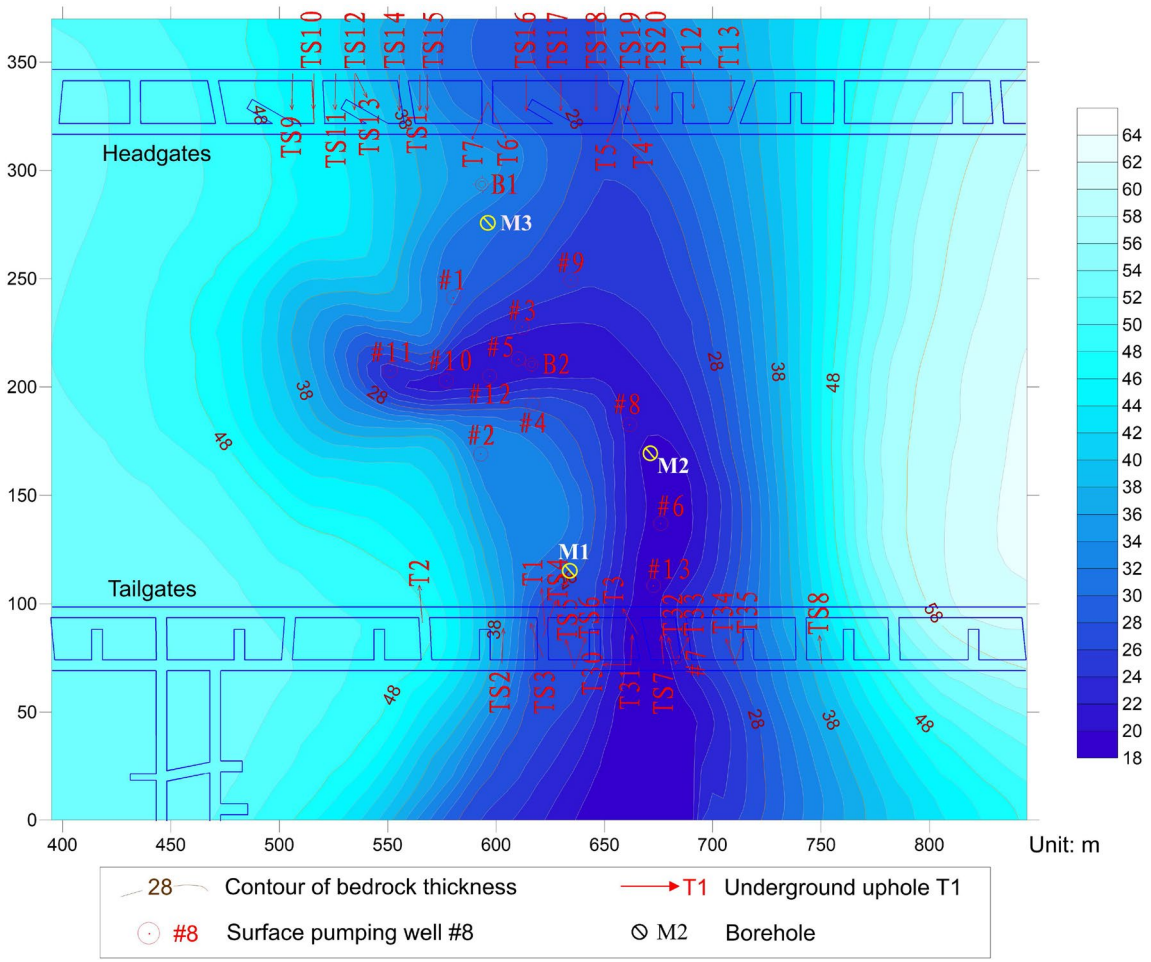

Fig. 7 The locations of wells and boreholes

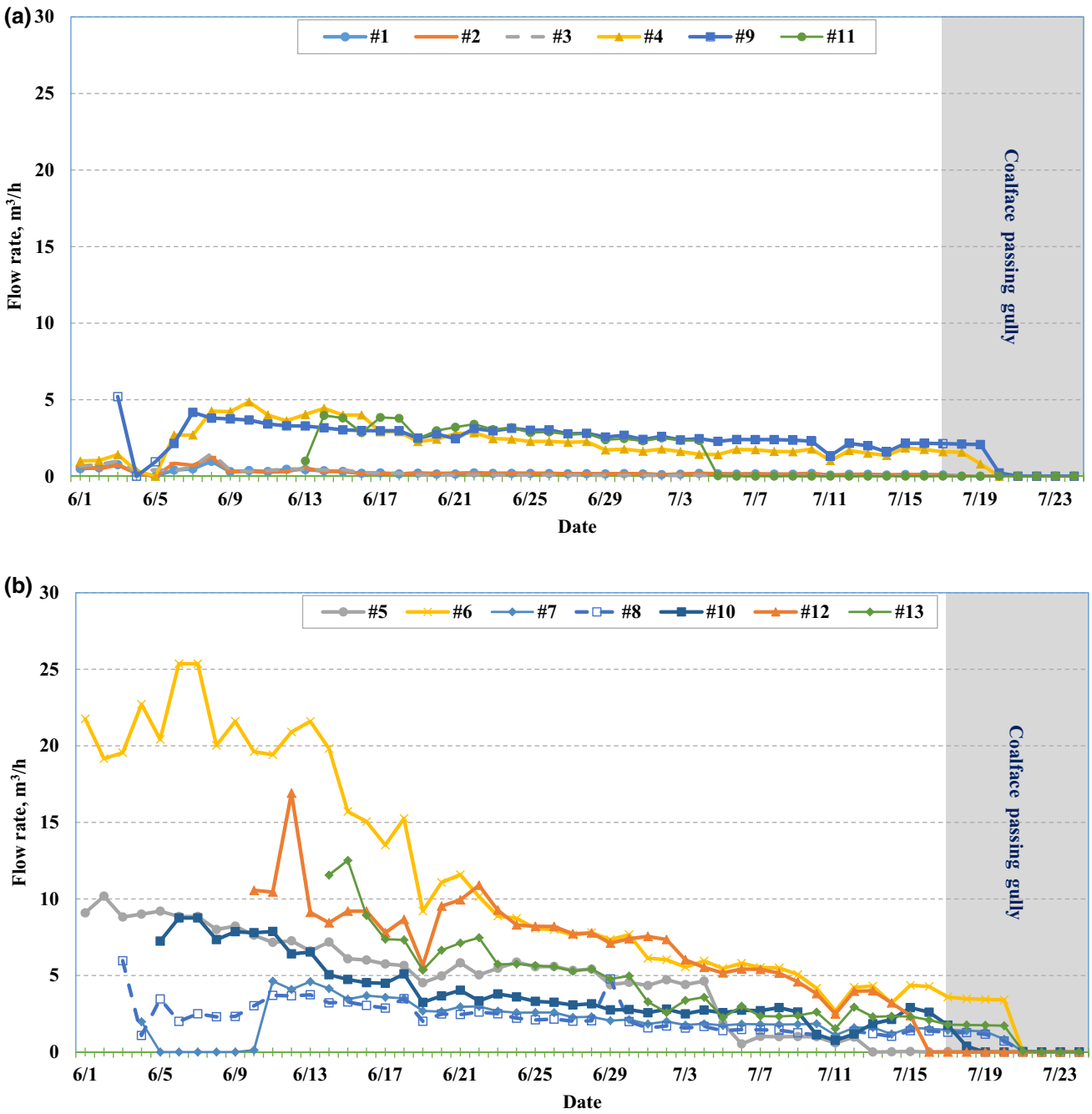

Fig. 8 The flow rates in the pumping wells: **a** the wells at the bottom; **b** the wells at the banks

Grouting

Borehole grouting is a proven geotechnical engineering technology for sealing substrata (Henn 1996; Warner 2004). The essence of using grouting to prevent groundwater inrush during mining is the formation of barrier covers in permeable or water-bearing layers (Kipko 1988).

After pre-mining aquifer dewatering, the remaining groundwater was mainly located at the bottom of the buried gully. The strata beneath the base of the buried gully is pretty thin, only 18.2 m thick at its thinnest, which is the most vulnerable sector. Although the water volume had been reduced to a small quantity, water inrush could still occur locally due to the presence of the thin rock strata. Therefore, grout was injected into the bottom of the sandy layer to create a consolidated zone and seal off the potential inrush pathways.

So 25 grouting holes were drilled from the ground surface to the bottom of the sandy layer in the gully bottom zone

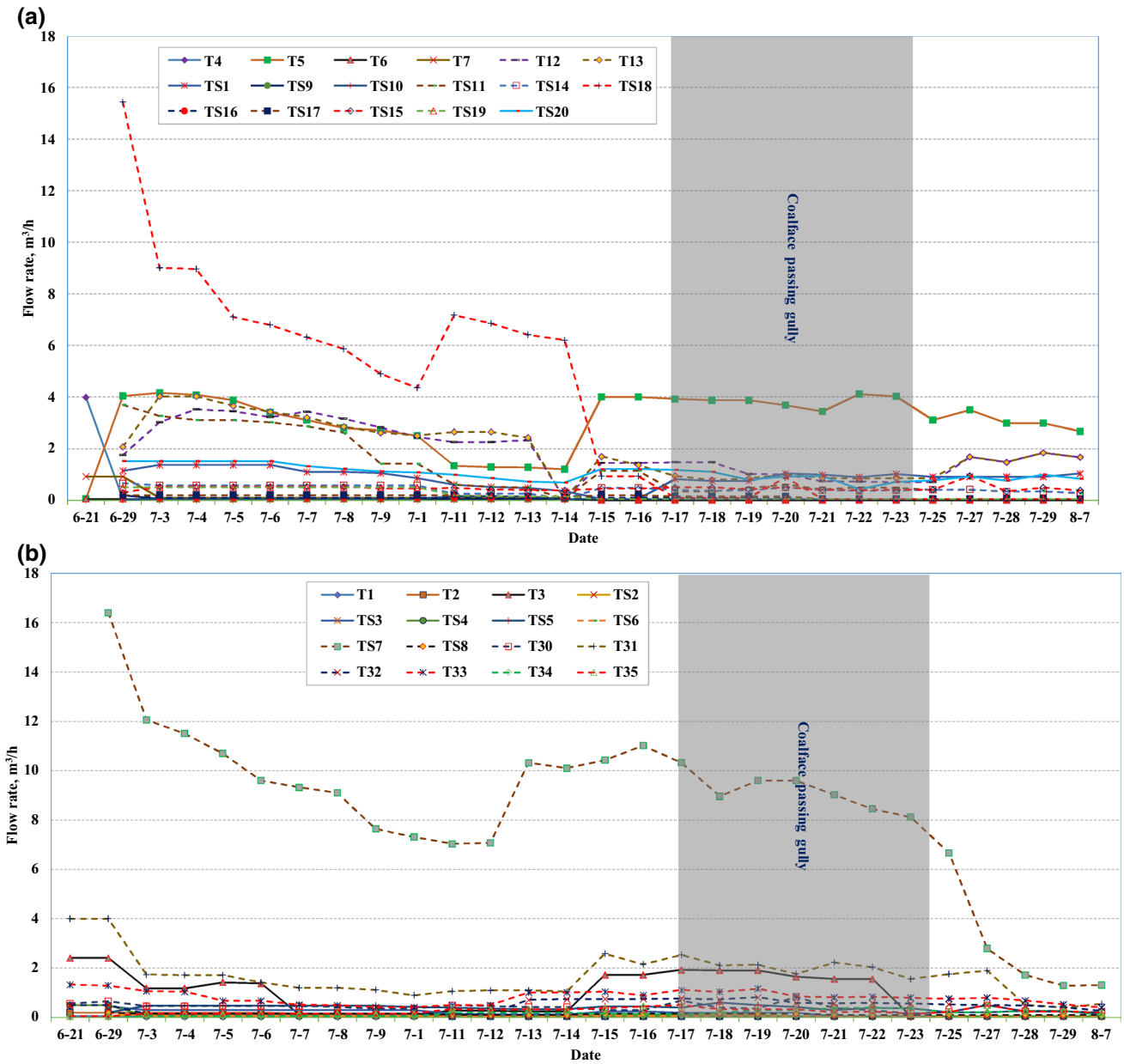

Fig. 9 The flow rates in the underground upholes: **a** the boreholes around the headgates; **b** the boreholes around the tailgates

where the bedrock was thinner than 20 m. The grout material was mainly mixed with Portland cement, quick-setting cement, sodium silicate, analytical reagent triethanolamine, and polyurethane.

Field Observations

Water Table

The actual aquifer thicknesses before and after pre-mining dewatering were collected (Fig. 10). The water table dropped about 1.5–13 m (5.21 m, on average). The aquifer thickness in the buried gully dropped 2–3 m from 14 to 16 m, and the calculated static-storage of the groundwater was 6054 m^3, which was safe for underground mining without risk of sand or water inrush after pre-dewatering and grouting.

Overburden Movement

Three boreholes, M1, M2, and M3, were placed near the tailgate, where the overburden strata was thinnest, and the headgate, respectively. The depths were 25, 35, and 25 m, respectively. The diameters were 170 mm in the

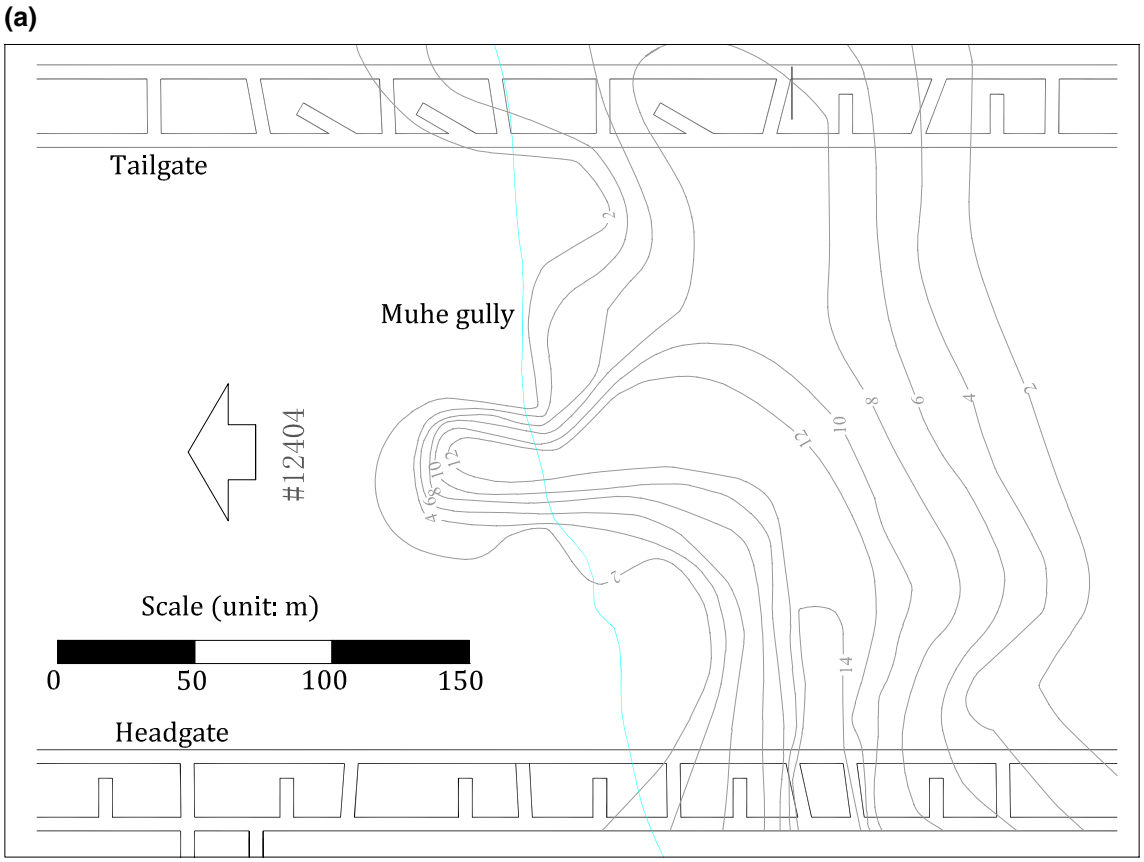

Fig. 10 The contour of aquifer thickness **a** before dewatering; **b** before coalface entering the gully zone

unconsolidated layers and 91 mm in the overburden. In the top unconsolidated layers, casings of 127 mm in diameter were installed. The water table and drilling fluid loses were logged to analyze the heights of the fractured and caved zones.

In borehole M1, there was no water backflow when it was drilled to a depth of 6.27 m, indicating that the borehole entered the fractured zone. At a depth of 26.92 m, there was no pressure on the drills, and rock core could not be collected, indicating that the borehole entered the caved zone. When the mining depth in borehole M1 was 40.25 m with a mining height of 3.6 m and a surface subsidence of 1.8 m, the heights of the fractured and caved zones were calculated to be 28.58 and 7.93 m, respectively.

In borehole M2, there was no water backflow when it was drilled to the depth of 26.37 m, indicating that the borehole entered the fractured zone. At the depth of 32.31 m, the drilling pressure decreased significantly, which means the borehole was located atop the caved zone. When the mining depth in borehole M2 was 50.35 m with a mining height of 3.5 m and surface subsidence of 2.1 m, the heights of the fractured and caved zones were calculated to be 18.38 and 12.44 m, respectively.

In borehole M3, there is no water backflow when it was drilled to the depth of 16.81 m, indicating that the borehole entered the fractured zone. At a depth of 25.28 m, the drilling pressure decreased significantly, which means the borehole reached the top of the caved zone. When the mining depth in borehole M2 was 43.93 m with a mining height of 3.5 m and a surface subsidence of 1.2 m, the heights of the fractured and caved zones were calculated to be 22.42 and 13.95 m, respectively.

Discussion and Conclusions

The modelled heights of the caved and fractured zones matched the field observations well. Both the UDEC modelling and field observation revealed that the overburden strata were heavily fractured. The ratio of the fractured zone to mining height ranged from 5.25 to 7.94. The fractured zone extends up to the top of the rock overburden, especially at the buried gully, and the thin strata could not prevent water or sand from flowing into the goaf without special treatment. Both the existing empirical assessments and numerical modelling results indicate that the overlying

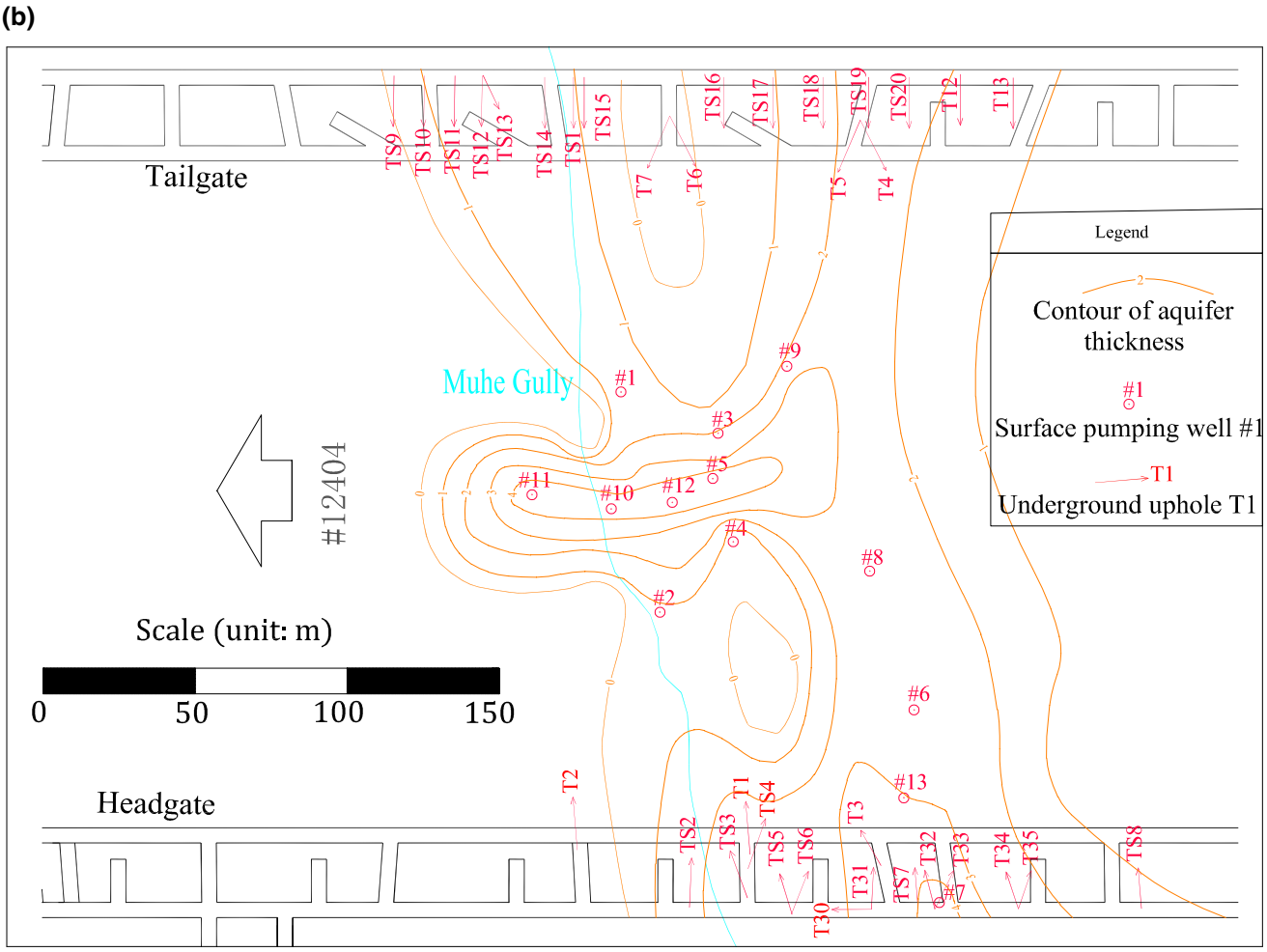

Fig. 10 (continued)

strata may be involved in the fractured zone and that the mining of panel #12,404 was in great risk of water and sand inrush, when the coalface was retreated near the gully zone.

Pre-mining dewatering was important in preventing the hazard of sand and water inrush. 13 pumping wells and 33 underground upholes were drilled to lower the water table or even removing the groundwater. Pumping volumes started to decrease when the coalface was 20–40 m away from the well, and the flow rate in the underground upholes started to increase when the coalface was 15–40 m away from the boreholes. Thus, the overburden fractures developing ahead of the coalface were gradually connected to the aquifer. As the coal face passed the gully, the pumping volume in the well approached zero and the flow rate in the underground upholes remained virtually constant, which means that the roof was totally fractured and that the water did not inrush into the goaf in a short time but rather seeped down along the fractures. Based on a flow rate analysis on the pumping wells and underground upholes, the wells or upholes located at the bottom of the gully were generally more effective on dewatering the aquifer than those located at the banks. Therefore, wells or upholes should be preferentially placed at the bottom of the gully.

The water depth in the buried gully was lowered ahead of mining by dewatering the aquifer, so that both the risk of water inrush and the initial driving force on the sand was reduced substantially. Grout injection was injected into the bottom of the buried gully to reduce sand liquidity and seal off the pathways for groundwater inrush. The field observations of the water table, underground water yield, and overburden movement demonstrate the validities of the above measures and the predictive method.

Acknowledgements We thank the National Natural Science Foundation of China (Grant 51504240), the National Key Basic Research Program of China (Grant 2015CB251600), Qing Lan Project (Grant Sujiaoshi (2016)15), the Fundamental Research Funds for the Central

Universities (2017XKZD07), and the Priority Academic Program Development of Jiangsu Higher Education Institutions (PAPD) for their financial support. The authors are also grateful for the helpful comments provided by the anonymous reviewers and the journal's editors.

References

Benko B, Stead D (1998) The Frank slide: a reexamination of the failure mechanism. Can Geotech J 35:299–311

Booth CJ (2002) The effects of longwall coal mining on overlying aquifers. Spec Publ Geol Soc Lond 198:17–45

Fan LM (1996) Controlling tecnological study onsuffosion hazard of coal shaftin shenfu minin area. Chin J Geol Hazard C 7:35–38 (Chinese)

Fan GW, Zhang DS, Zhai DY, Wang X, Lu X (2009) Laws and mechanisms of slope movement due to shallowly buried coal seam mining under ground gully. J Coal Sci Eng (China) 15:346–350

Gandhe A, Venkateswarlu V, Gupta RN (2005) Extraction of coal under a surface water body—a strata control investigation. Rock Mech Rock Eng 38:399–410

Henn RW (1996) Practical guide to grouting of underground structures. American Soc of Civil Engineers, Reston, VA

Kendorski FS (1993) Effect of high-extraction coal mining on surface and ground waters. In: Peng SS (ed) Proc, 12th International Conf on Ground Control in Mining, Morgantown, WV, pp 228–235

Kendorski FS (2006) Effect of full-extraction underground mining on ground and surface waters a 25-year retrospective. In: Peng SS (ed) Proc, 25th International Conf on Ground Control in Mining, Morgantown, WV, pp 425–430

Kesserû Z (1995) New Approaches and results on the assessment of risks due to undermining for mine's safety and for protecting of water resources. Proc, International Conf on Water Resources at Risk, International Mine Water Assoc (IMWA), Denver, pp 53–72

Kipko EJ (1988) Application of grouting techniques for the solution of environmental problems during mining. In: Proc, 3rd International Mine Water Congress. Australasian Inst of Mining and Metallurgy, Melbourne, pp 655–666

Lai XP, Shan PF, Cai MF, Ren FH, Tan WH (2015) Comprehensive evaluation of high-steep slope stability and optimal high-steep slope design by 3D physical modeling. Int J Miner Metall Mater 22:1–11

Li G, Zhou W (2006) Impact of karst water on coal mining in North China. Environ Geol 49:449–457

Li WP, Sun R, Wang W, Zhang Z, Zhao X (2002) Study on the height of water flowing fractured zone formed by shallow coal mining in yu-shen-fu mine area of north shaanxi province and its environment-ecology sig-nificance. J Eng Geo 10:153–156

Liu T (1981) Surface movements, overburden failure and its application. Coal Industry Press, Beijing

Marschalko M, Treslin L (2009) Impact of underground mining to slope deformation genesis at Doubrava Ujala. Acta Montan Slovac 14:232–240

Miao XX, Cui X, Wang JA, Xu JL (2011) The height of fractured water-conducting zone in undermined rock strata. Eng Geol 120:32–39

Morsy K, Peng S (2002) Numerical modeling of the goaf loading mechanism in longwall coal mines. In: Peng SS (ed) Proc, 21st International Conf on Ground Control in Mining, Morgantown, pp 58–67

Morton KL, Van Mekerk F (1993) A phased approach to mine dewatering. Mine Water Environ 12:27–33

National Coal Board (1975) Subsidence Engineers' Handbook. Mining Dept, UK National Coal Board, London

Peng SS (2008) Coal mine ground control. 3rd edit, Published by Syd S Peng, Morgantown, WV

Qian MG, Miao XX, He FL (1994) Analysis of key block in the structure of voussoir beam in longwal mining. J Chin Coal Soc 19:557–563

Qian MG, Miao XX, Xu JL (1996) Theoretical study of key stratum in ground control. J Chin Coal Soc 21:225–230

Saeedi G, Shahriar K, Rezai B (2013) Estimating volume of roof fall in the face of longwall mining by using numerical methods. Arch Min Sci 58:767–778

Singh R (1986) Mine inundations. Int J Mine Water 5:1–28

Singh R, Atkins A (1983) Design considerations for mine workings under accumulations of water. Int J Mine Water 1:35–56

Stead D, Benko B (1998) The influence of underground workings on slope instability mechanisms. In: Moore D, Hungr O (eds) Proc, 8th International Congress International Assoc for Engineering Geology and the Environment. A A Balkema, Vancouver, pp 1493–1500

Tammetta P (2013) Estimation of the height of complete groundwater drainage above mined longwall panels. Groundwater 51:723–734

Tang F (2009) Research on mechanism of mountain landslide due to underground mining. J Coal Sci Eng (China) 15:351–354

Tieman GE, Rauch HW (1987) Study of dewatering effects at an underground longwall mine site in the Pittsburgh seam of the northern Appalachian coalfield. Proc, USBM IC 9137, Pittsburgh. pp 72–89

Wang XF, Zhang DS, Fan GW, Zhang CG (2011) Underground pressure characteristics analysis in back-gully mining of shallow coal seam under a bedrock gully slope. Min Sci Technol (China) 21:23–27

Wang XF, Zhang DS, Zhang CG, Fan GW (2013) Mechanism of mining-induced slope movement for gullies overlaying shallow coal seams. J Mt Sci 10:388–397

Warner J (2004) Practical handbook of grouting: soil, rock, and structures. Wiley, New York City

Wu YP, Lu MS (2004) Analysis of sand inrush generation condition in coal mining of shallow coal seam. Mine Pressure Roof C 21:57–61 (Chinese)

Wu Q, Zhou W (2008) Prediction of groundwater inrush into coal mines from aquifers underlying the coal seams in China: vulnerability index method and its construction. Environ Geol 56:245–254

Zhang JC, Peng SP (2005) Water inrush and environmental impact of shallow seam mining. Environ Geol 48:1068–1076

Zhang X, Sanderson D (1998) Numerical study of critical behaviour of deformation and permeability of fractured rock masses. Mar Petrol Geol 15:535–548

Zhang J, Shen B (2004) Coal mining under aquifers in China: a case study. Int J Rock Mech Min Sci 41:629–639

Zhang DS, Fan GW, Wang XF (2012) Characteristics and stability of slope movement response to underground mining of shallow coal seams away from gullies. Int J Min Sci Technol 22:47–50